Energy Signatures and Production Process Information

Giuseppe Fanizza*, Alessandro Massaro, *Senior Member IEEE*, and Giuseppe Starace

***Abstract*— This paper proposes an innovative methodology to define the energy signature and traceability of a company producing agro-textiles from purposely extruded yarns and films. In the proposed analytical approach, Fourier analysis is applied to extract energy-related information. The analysis makes it possible to interpret the results in both the frequency and time domains, identifying interpretative features associated with energy consumption and balancing in yarn manufacturing. Dominant spectral components were consistently observed below 25 cycles/day, accounting for the majority of recurrent energy variability, while intermediate bands between 10-25 cycles/day exhibited amplitudes between 5% and 10% of the daily mean consumption. High-frequency components above 60 cycles/day were found to contribute less than 1–5% and were largely transient. The paper identifies key aspects for interpreting the energy signatures of the analyzed production lines and proposes a tentative protocol for implementing a data-driven approach to production-process monitoring and corrective action. A further possible outcome of the proposed analytical method is its application to manufacturing industries in other sectors.**

I. INTRODUCTION

Interfaces depicting the raw sensor outputs or graphs coming from data elaboration are versatile tools able to monitor energy performance in manufacturing lines [1] as well as in production buildings [2]. The use of monitoring sensors is fundamental to extract the power signature of manufacturing units, finding corresponding energy usage in real time to identify anomalous operation conditions [3], [4]. Recently, some researchers studied multivariate statistical approaches to extract information and energy signatures from industrial processes [5]. The estimation of energy indicators makes it possible to model complex energy ecosystems [6] thus facilitating the creation of energy digital twin (DT) models [7], [8], [9], [10], [11], [12] also incorporating artificial-intelligence-based data-analysis approaches [13], [14]. Focusing the attention on the agro-textile sector, energy monitoring has been analyzed with a focus on general site-management aspects [15], [16] rather than on detailed manufacturing processes. This leaves open a specific scientific issue: the lack of compact, reproducible descriptors able to link long-term energy measurements with the recurrent dynamics of a production line. In particular, existing monitoring approaches often identify consumption levels or anomalies, but they do not explicitly decompose the energy signal into stable and transient components that can be interpreted as a process signature. The contribution of this paper is therefore threefold: (i) to define a Fourier-based recurrence analysis for irregular industrial energy data, (ii) to separate dominant production-related oscillations from short-term fluctuations by means of absolute and normalized cutoffs, and (iii) to translate the resulting energy signature into a monitoring protocol suitable for corrective actions and future digital-twin implementation.

Yarn manufacturing was selected as a representative case study because extrusion is a continuous, energy-intensive process in which heating, stretching, cooling, lubrication, and winding phases operate simultaneously and generate recurrent energy patterns. Although the experimental validation is focused on this industrial line, the proposed procedure is not specific to polyethylene yarns: it can be transferred to other continuous or semi-continuous manufacturing processes equipped with time-resolved energy meters.

The agro-textile manufacturing process can be divided into two macro areas:

- Spinning Area (yarn and film manufacturing);
- Weaving Area.

The raw material for the production of monofilaments is high-density polyethylene (HDPE) (a thermoplastic polymer), supplied in granules by various manufacturers, which are mixed, according to specific formulations, with additives and stabilizers in order to obtain the desired physical and mechanical-resistance characteristics. The process of yarn manufacturing consists in aggregating the parts of the raw material, through a procedure carried out exclusively by a continuous extrusion line made up of several machines or mechanical parts placed in sequence. The technological

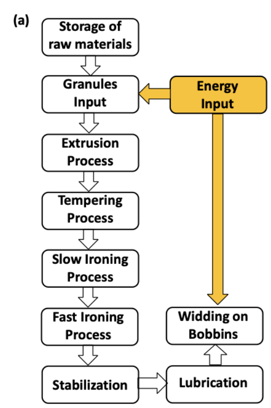

Fig. 1. Block diagram sketching the yarn manufacturing (spinning process).

production cycle of yarn manufacturing of Fig. 1 is better

*Corresponding author: fanizza@lum.it

All authors are with Department of Engineering of LUM "Giuseppe Degennaro" University, Strada Statale 100 km 18, Casamassima, 70010 Bari, Italy.

described by the following steps:

- Phase 1: Storage and subsequent loading of the raw material (HDPE granules with the necessary additives according to production requirements) into the screw extruder;
- Phase 2: Extrusion of first-stage yarns through dies. This process reaches approximately 230°C and 10 bars due to friction and heating power;
- Phase 3: Cooling and hardening in water tank at 10°C to reach the first desired shape of the yarns;
- Phase 4: First forming step of the yarns by heated stretching in a water oven at approximately 98°C;
- Phase 5: Air cooling of yarns using forced air at room temperature;
- Phase 6: Stabilization of the yarns in their final shape by heated stretching in an air oven at approximately 98°C;
- Phase 7: Yarn lubrication to prepare for winding and remove electric charges;
- Phase 8: Winding of spools for subsequent processes (such as textile production on looms).

Fourier analysis was selected because the objective is not only to detect isolated peaks, but also to identify recurrent time scales in a long energy-consumption signal. Compared with a direct time-domain inspection, the frequency-domain representation makes it possible to distinguish slow daily modulations, sub-diurnal production oscillations, and high-frequency transients using a limited number of interpretable coefficients. Up to now, Fourier analysis has been used mainly for defect analysis and not for interpreting energy consumption data of a manufacturing production line [17], [18], [19]. Some studies used Fourier power spectra to reproduce machining processes [20], thus suggesting the possibility of extracting process-related information from energy consumption. The novelty of the present work is the use of daily Fourier coefficients as an energy-signature descriptor and as the basis for a practical monitoring workflow.

II. Method

The original dataset consists of the time series of the energy consumption along a given production line without the UPS system. The same procedure was also checked on an additional dataset including the UPS contribution, in order to verify that the dominant spectral trends were not an artifact of a single acquisition configuration. The raw dataset is organized as a collection of points where the first entry is the time interval Δt_k [s] between consecutive observations and the second entry, x_k, is the value of the dissipated energy at that time. The sampling in the time domain is irregular; therefore, direct indexing by measurement number does not correspond to uniform time spacing. To reconstruct a more uniform temporal structure of the dataset, a cumulative sum of the intervals is then performed as follows:

$$t_k = \sum_{j=1}^{k} \Delta t_j. \tag{1}$$

This operation produces a strictly increasing sequence of observation times $\{t_k\}$, from which the measurement pairs (t_k, x_k) are obtained. For convenience, the times are normalized in units of days,

$$t_k^{(\text{day})} = \frac{t_k}{86400}, \tag{2}$$

allowing direct comparison with natural daily cycles.

Since the signal is both noisy and irregularly sampled, the first processing stage aims to produce a locally smoothed and more homogeneous representation. For each observation time t_k, a neighborhood of points within a fixed temporal window Δt is considered. In the tests reported here, a 5-minute averaging window was used because it corresponds to the minimum stable acquisition interval of the monitoring system; wider windows can be used when the objective is to suppress short-term machine transients:

$$W_k = \{i \mid |t_i - t_k| \leq \Delta t\}. \tag{3}$$

The data within this window are averaged to obtain a moving average:

$$\bar{x}(t_k) = \frac{1}{|W_k|} \sum_{i \in W_k} x_i. \tag{4}$$

This operation smooths out high-frequency fluctuations smaller than the window width while preserving slower modulations such as diurnal or sub-diurnal trends. The result is a filtered dataset $\{t_k^{(\text{day})}, \bar{x}(t_k)\}$, which maintains the original time resolution but with reduced noise and redundancy.

At this point, the discrete dataset is interpolated using the continuous function $g(t)$, in order to perform a Fourier analysis in the frequency domain. Then, to study the evolution of spectral content over time, the interpolated signal is analyzed within consecutive one-day intervals. For each integer day d, a local Fourier transform is computed:

$$C_n(d) = \int_d^{d+1} g(t)\, e^{2\pi i n (t-d)}\, dt, \tag{5}$$

where n is an integer index corresponding to the harmonic frequency in cycles per day (c/d). Positive n values represent oscillations with frequencies n c/d, while negative n correspond to their complex conjugates. In practice, n is truncated to $|n| \leq 120$, i.e. at the 120th fraction of a day, roughly 10 minutes. This step produces, for each day, d, a discrete spectrum $\{C_n(d)\}$ that captures both the amplitude and phase of the periodic components present in the signal over that 24-hour interval.

The modulus of each Fourier coefficient,

$$P_n(d) := |C_n(d)| = \sqrt{(\operatorname{Re} C_n(d))^2 + (\operatorname{Im} C_n(d))^2}, \tag{6}$$

represents the amplitude of the n-th harmonic during day d. Tracking $P_n(d)$ as a function of time allows one to study how specific frequencies strengthen or weaken across the dataset.

To quantify how often certain harmonics dominate, two thresholding criteria are introduced. First, a series of absolute amplitude thresholds P_{th} is used (e.g., 0.8, 1.0, 1.2 in the same amplitude units as the signal). For each threshold, all pairs (n, d) satisfying $P_n(d) \geq P_{\text{th}}$ are collected, and the frequency indices n are tallied to build histograms. These histograms show how frequently each harmonic exhibits significant amplitude throughout the observation period and thus provide a statistical measure of spectral recurrence. Second, normalized thresholds are defined as fixed percentages of the zero-frequency coefficient $C_0(d)$, which represents the daily mean level. This makes the procedure less dependent on the absolute magnitude of the signal and improves comparability across production lines or product recipes.

To conclude, we remark that our cutoff framework can be tested against its effectiveness by reconstructing the signal from the obtained coefficients. For any day d, a truncated Fourier series is formed:

$$\tilde{g}_d(\tau) = \sum_{n=-N}^{N} C_n(d) e^{-2\pi i n \tau}, \qquad \tau = t - d \in [0,1]. \tag{7}$$

If the interpolation and Fourier decomposition are well-behaved, $\tilde{g}_d(\tau)$ closely matches the original function $g(t)$ over that same day. The comparison between the interpolated signal and its truncated Fourier reconstruction provides a qualitative analysis of how much the overall signal is affected by the discarded frequencies. Moreover, an analogous form of Eq. (7) can be obtained also by limiting the chosen spectrum to those frequencies whose amplitude is greater than P_{th}, leading to the truncated reconstruction $\tilde{g}_d^{\text{th}}(\tau)$ in the time domain.

In the next section, we present the results of the analysis for a selected production line and discuss the most recurrent peaks within it. The proposed protocol can then be repeated on different production lines or production recipes in order to identify shared spectral patterns and line-specific deviations in energy consumption.

III. Results and Discussion

The recurrence histograms in Fig. 2 summarize the frequency content of the reconstructed signal across the entire 345-day observation period. Each histogram counts, for each frequency bin, the number of days in which the amplitude of a given harmonic exceeded a fixed threshold, according to the procedure described above. First, three amplitude levels were considered: 0.8, 1.0, and 1.2 in normalized units, represented by red, green, and blue, respectively. These absolute thresholds are introduced as exploratory cutoffs and are not intended as physically universal parameters. For this reason, Section 3.1 introduces a normalized thresholding strategy based on percentages of the zero-frequency mode, which removes dependence on absolute signal magnitude and improves cross-dataset comparability. These distributions provide a compact, cumulative view of how often each harmonic emerged as dynamically significant.

The spectra exhibit a pronounced concentration of recurrences at low frequencies, with a sharp maximum at ~ 10 c/d. The 5-minute window corresponds to the minimum stable sampling interval of the monitoring system and allows detection of sub-hourly machine adjustments. The first informative peak emerges roughly at 10 c/d and indicates the presence of broad quasi-periodic structures with characteristic timescales of a few hours.

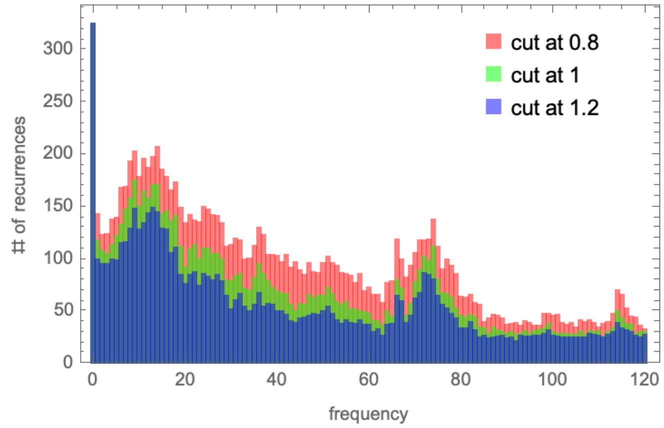

Fig. 2. Recurrence histogram of harmonic frequencies for a 5-minute averaging window. Each color indicates the number of days in which the harmonic amplitude exceeded a given threshold (red: 0.8, green: 1.0, blue: 1.2).

Beyond this baseline regime, a secondary cluster of enhanced recurrence approximately in the 15–20 c/d is observed. This region corresponds to sub-diurnal oscillations, whose persistence over many days suggests an underlying modulation with characteristic times between about one and two hours. The fine structure within this band, visible as local maxima separated by a few c/d, likely arises from intermittent, short-duration events with slightly different periodicities. Such variability is consistent with systems in which rapid transient processes coexist with slower background variations. At higher frequencies, the recurrence count decreases steadily, approaching a uniform low level beyond 80 c/d. The absence of coherent peaks in this range indicates that residual high-frequency fluctuations are mainly stochastic noise rather than systematic periodic components. Nevertheless, some increase in recurrence counts remains visible near 60-80 c/d, which may correspond to the residual signatures of instrumental cycles or processing artifacts that survive the smoothing stage.

The relative amplitudes across the three threshold cuts show that the qualitative spectral pattern is robust: the same peaks remain visible even as the cutoff is raised from 0.8 to 1.2, with only the overall counts decreasing. This indicates that the detected harmonics are not dominated by random fluctuations but correspond to genuinely recurrent features of the signal. The monotonic decay in recurrence with increasing frequency further supports the interpretation that most of the spectral power is concentrated in the low- and mid-frequency bands.

Overall, these histograms reveal that the system under study is characterized by a hierarchical frequency structure: a persistent low-frequency background reflecting slow trends, a stable intermediate band corresponding to reproducible sub-diurnal oscillations, and a rapidly decaying high-frequency tail dominated by transient noise. The comparison between the two smoothing scales demonstrates that the method reliably captures the invariant spectral content of the signal while allowing quantitative assessment of how smoothing affects the visibility of short-period fluctuations.

A. Normalized Cutoff Reconstruction Tests

To visualize the effect of the normalized spectral cutoff in the time domain, the daily signal was reconstructed using only the Fourier modes with amplitudes exceeding a fixed percentage of the 0-th harmonic (mean level). It should be recalled that three thresholds were considered: 1%, 5%, and 10%. Fig. 3 shows the corresponding reconstructions (red, green, and blue curves, respectively) compared with the original interpolated signal (gray dashed line) for the 5-minute averaged dataset.

The 1% reconstruction (red) reproduces nearly the entire structure of the original signal, including high-frequency oscillations and fine-scale variability. The agreement is excellent across all phases of the day, with the reconstructed curve following the detailed peaks and troughs of the reference waveform with high accuracy. This demonstrates that the Fourier representation is complete and that the weak, high-order harmonics below the 1% threshold collectively account for only a minor correction to the total signal.

At the intermediate threshold of 5% (green), the reconstruction remains faithful to the main envelope but exhibits noticeable smoothing of small-scale features. Rapid fluctuations with characteristic timescales below about 30–60 minutes are attenuated, while broader diurnal modulations are preserved. This filtering behavior confirms that harmonics with amplitudes between 1% and 5% of the mean level correspond primarily to transient, short-lived variations rather than to persistent oscillatory components. The resulting curve offers a compact, noise-reduced representation of the signal that retains its essential temporal morphology. When the cutoff is raised to 10% (blue), the reconstruction becomes markedly smoother, reducing to a slowly varying trend that tracks the average daily modulation. In this case, only the most powerful and stable modes contribute, effectively isolating the long-term component of the variability. The 10% reconstruction captures the general diurnal pattern but omits higher-frequency oscillations entirely. The gradual curvature of the resulting waveform reflects the strong dominance of the lowest Fourier modes and illustrates how the normalized cutoff can be used as a tunable spectral filter.

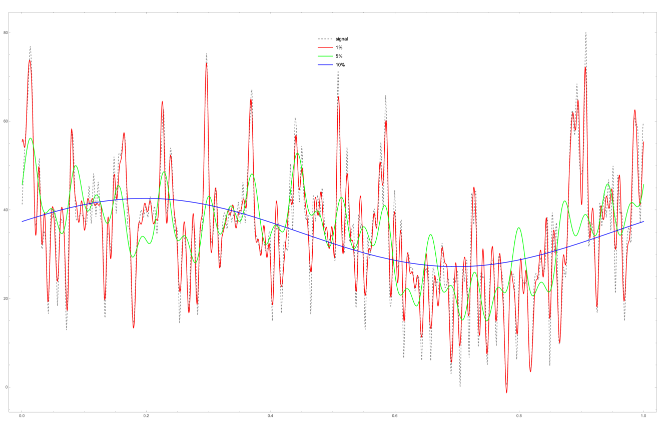

Fig. 3. Reconstructed signal for day 200 using normalized spectral cutoffs defined as 1%, 5%, and 10% of the zeroth-mode amplitude for the 5-minute averaged dataset. The 1% reconstruction (red) reproduces the full structure of the signal, while the 5% (green) and 10% (blue) cutoffs progressively smooth high-frequency fluctuations, isolating the dominant diurnal trend.

Overall, the normalized cutoff reconstructions demonstrate that the daily waveform is spectrally compact. A small subset of harmonics exceeding 5–10% of the mean amplitude is sufficient to capture the main daily modulation, while weaker components below the 1% level refine the shape with higher-frequency detail. The close agreement between the 1% reconstruction and the original signal validates the accuracy of the sliding Fourier decomposition and confirms that most of the physical variability is contained within a limited range of harmonics. These normalized reconstructions confirm that the Fourier-based decomposition is both efficient and physically interpretable. Adjusting the cutoff percentage acts as a controlled spectral filter: low percentages retain the complete signal, while higher values isolate the most significant harmonics. The stability of the waveform shape across all thresholds highlights the robustness of the method and underscores that a small set of dominant modes encapsulates the essential daily dynamics of the system.

B. Comparison Between Absolute and Normalized Cutoff Spectra

A direct comparison between the absolute- and percentage-based cutoff analyses reveals a consistent spectral hierarchy, yet with important nuances in the representation of secondary harmonics. Both methods identify a dominant concentration of recurrent power at low frequencies (below $\sim$25 c/d), corresponding to the slow diurnal and sub-diurnal modulations that define the overall temporal structure of the signal. However, the normalized cutoff framework clarifies the relative energy-related importance of these modes by scaling them to the mean level of the signal, allowing a more quantitative distinction between stable, high-power harmonics and the weaker, transient ones.

In the absolute-threshold histograms, secondary peaks are observed near 70-80 c/d and, more prominently, around 120 c/d. These features persist even as the amplitude cutoff increases, suggesting that they correspond to genuine, albeit intermittent, components of the signal rather than noise artifacts.

The 70-80 c/d region likely represents short-period oscillations with characteristic timescales of 15–20 minutes, while the narrow feature near 120 c/d corresponds to a $\sim$12-minute modulation. Such high-frequency peaks appear more clearly in the finer 5-minute averaging, indicating that they are sensitive to the temporal resolution of the dataset.

When the normalized thresholds are applied, these secondary peaks become much less pronounced above the 5% level and almost vanish at 10%. This behavior indicates that their amplitude contribution rarely exceeds a few percent of the mean daily signal, confirming their transient or low-energy nature. Nonetheless, their recurrence at the

1% threshold suggests that they represent real fluctuations superimposed on the dominant daily cycle, possibly arising from high-frequency processes or instrumental variability. The smooth suppression of these peaks with increasing normalized cutoff also validates the internal consistency of the Fourier decomposition: as the selection criterion becomes more stringent, only the strongest and most stable harmonics remain.

Overall, the comparison demonstrates that both cutoff schemes highlight the same underlying structure (a strong, compact low-frequency core accompanied by weaker high-frequency sidebands) but differ in how they express the balance between persistent and transient features. The absolute thresholds emphasize recurrence, capturing even low-power harmonics that reappear intermittently across days, whereas the normalized cutoffs quantify the energy contribution of each component relative to the mean level. The coexistence of both views provides a complete description of the signal: a robust diurnal foundation modulated by occasional short-period oscillations that contribute minimally to the overall power budget but may encode subtle dynamical variations.

IV. Discussion: Data Interpretation and an Energy-Signature Protocol for Data-Driven Procedures

The proposed energy signature analysis supports the interpretations summarized as follows. Since detailed production logs were not available for publication, the association between spectral components and plant events is interpreted at the level of process phases and operating regimes rather than through a one-to-one labelled validation. Nevertheless, the extrusion line provides a clear physical basis for this interpretation: heating and stretching stages are expected to contribute to slow and stable components, while regulation actions, winding variations, and machine transients are expected to appear as short-period oscillations.

- Production peaks in Fig. 2. By considering the data analysis of Fig. 2, additional high-frequency peaks can be distinguished, showing that production is subject to short-term energy fluctuations, as occurs during continuous machine setting and regulation. Controlling these fluctuations makes it possible to balance machine settings and reduce energy consumption by decreasing losses caused by machine transients.
- Daily signal (Fourier reconstruction) in Fig. 3. The daily signal reconstruction allows the dominant diurnal energy trend to be isolated from oscillations. The daily cleaned trend represents the average daily signature (average energy consumption), whereas the ripples indicate the unnecessary energy overloads that should be controlled. Strong oscillations could also indicate an initial machine failure condition leading to product defects.

The data interpretation in the bullet points above indicates a procedure for reading energy values and defining a monitoring guideline protocol. Business Process Model and Notation (BPMN) workflows are useful to standardize

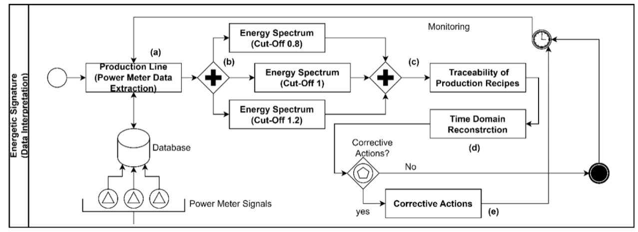

Fig. 4. BPMN workflow summarizing the phases of energy-signature interpretation (guideline protocol).

measurement procedures [21]. In the proposed paper, the same graphical notation was used to structure the workflow in Fig. 4, summarizing the guideline protocol to interpret the energy signature and integrate data analysis into an efficient energy monitoring system. The workflow is structured in the following main phases:

- Phase (a): data acquired from the power meters of the specific production line and extracted from a database covering the whole supply chain are analytically processed;
- Phase (b): Fourier analysis is performed by applying different cutoffs;
- Phase (c): the interpretation of the results from Phase (b) makes it possible to compare production formulations associated with different product types and to identify deviations from the expected spectral profile;
- Phase (d): the time-domain signal is reconstructed using the Fourier coefficients, enabling analysis of signal noise interpreted as energy fluctuations around an average value;
- Phase (e): if the fluctuations are strong, possible corrective actions are evaluated to decrease the unnecessary consumption of energy.

The objective of this study is methodological: to demonstrate that a Fourier-based recurrence analysis can be used to extract physically interpretable energy signatures from long-term industrial energy measurements. Direct validation against detailed production logs, maintenance records, or labelled anomalies was not feasible within the constraints of industrial data confidentiality and is therefore outside the scope of the present work. For this reason, the present interpretation should be considered a process-oriented reading of the spectral features, not yet a supervised diagnosis of specific plant events. Nevertheless, the internal validation provided by (i) consistency across two independent datasets (UPS off/on), (ii) robustness to the smoothing scale, and (iii) high-fidelity time-domain reconstruction demonstrates the internal coherence and physical plausibility of the proposed approach. Future work will explicitly incorporate production metadata to enable supervised validation and benchmarking. In a digital-twin perspective, the Fourier coefficients can act as compact state variables describing the energetic behaviour of the line: deviations from the expected coefficient pattern may then trigger alerts, update process models, or support predictive-maintenance decisions.

V. Conclusion

This paper discusses an innovative methodological approach based on the analytical processing of the energy consumption monitored in the frequency and time domains. The analysis was performed by processing the annual data from a company producing agro-textiles using extruded polyethylene yarns and films. The analysis shows that more than 70% of the recurrent spectral energy content is concentrated below 25 c/d, corresponding to stable production regimes, while fluctuations in the 10–25 c/d range typically account for 5–10% of the daily mean energy consumption. High-frequency components above 60 c/d were consistently below 5% and are attributable to transient machine adjustments or measurement noise. These quantitative findings confirm that the energy signature of yarn extrusion lines is spectrally compact and dominated by a limited set of reproducible harmonics. The proposed approach identifies characteristic intervals in the time domain in which power consumption peaks. This lays the foundation for a new framework for quantitatively analyzing which industrial operations lead to these peaks, in order to reduce possible undesired dissipation along the production line. A systematic identification based on synchronized production logs will be investigated in a forthcoming study. Although the case study concerns HDPE yarn extrusion, the method can be generalized to other continuous manufacturing contexts in which energy meters provide long time series and the process is characterized by recurrent operating cycles. In such settings, the same workflow can be used to define reference spectra, compare product recipes, detect deviations, and support corrective actions. The discussed theoretical approach may also represent a foundational concept for a digital twin model matching energy consumption with production processes, where the Fourier coefficients become compact indicators of the energetic state of the plant. Future work will focus on the quantification of key performance indicators and the integration of artificial intelligence tools supporting predictive maintenance and failure classification due to anomalous energy consumption.

Acknowledgment

This work was carried out using data extracted from the monitoring system installed in the whole manufacturing site and in particular on the yarn extrusion lines of Arrigoni Spa in its industrial plant of Putignano (Italy). The authors thank Paolo Arrigoni, Giuseppe Dimaggio and Marco Lippolis for their valuable support in strongly encouraging the analysis, making available real data and extracting them in a format suitable for elaboration. This has provided the basis for a productive and stable collaboration on the topic, that was deemed capable of adding value to the company's growth in terms of social, environmental and financial impacts.

References

[1] A. D. Rocha, N. Freitas, D. Alemão, M. Guedes, R. Martins, and J. Barata, "Event-driven interoperable manufacturing ecosystem for energy consumption monitoring," *Energies*, vol. 14, no. 12, p. 3620, 2021.

[2] N. Frigerio, A. Matta, and M. Rasella, "Energy monitoring of manufacturing plants: A real case application," *Procedia CIRP*, pp. 770–775, 2022.

[3] Y. Ren and G.-P. Li, "A contextual sensor system for non-intrusive machine status and energy monitoring," *Journal of Manufacturing Systems*, vol. 62, pp. 87–101, 2022.

[4] N. Panten, E. Abele, and S. Schweig, "A power disaggregation approach for fine-grained machine energy monitoring by system identification," *Procedia CIRP*, vol. 48, pp. 325–330, 2016.

[5] A. Amoresano, M. Barrasso, and G. Quaremba, "Multivariate statistical control of energy signatures in brewery production process," *Journal of Physics: Conference Series*, vol. 3143, p. 012101, 2025.

[6] A. Massaro and G. Starace, "Advanced and complex energy systems monitoring and control: A review on available technologies and their application criteria," *Sensors*, vol. 22, no. 13, p. 4929, 2022.

[7] M. Zeynivand, P. Esmaili, L. Cristaldi, and G. Gruosso, "A novel approach to digital twin-based energy efficiency monitoring and failure analysis in industrial applications," *Journal of Manufacturing Systems*, vol. 83, pp. 612–625, 2025.

[8] H. Li *et al.*, "Data-driven hybrid petri-net based energy consumption behaviour modelling for digital twin of energy-efficient manufacturing system," *Energy*, vol. 239, p. 122178, 2022.

[9] A. Rubio-Rico, F. Mengod-Bautista, A. Lluna-Arriaga, B. Arroyo-Torres, and V. Fuster-Roig, "The industrial digital energy twin as a tool for the comprehensive optimization of industrial processes," *Processes*, vol. 11, no. 8, p. 2353, 2023.

[10] H. Pruvost, F. Forns-Samso, O. Gnepper, and O. Enge-Rosenblatt, "Integrating energy system monitoring and maintenance services into a bim-based digital twin," in *Proceedings of the 49th Annual Conference of the IEEE Industrial Electronics Society (IECON)*, Singapore, 2023, pp. 1–6.

[11] D. Perossa, R. F. B. Santacruz, R. Rocca, and L. Fumagalli, "Digital twin application to energy consumption management in production: A literature review," in *Product Lifecycle Management. PLM in Transition Times*, ser. IFIP Advances in Information and Communication Technology. Cham: Springer, 2023, vol. 667.

[12] A. Billey and T. Wuest, "Energy digital twins in smart manufacturing systems: A literature review," *Manufacturing Letters*, vol. 35, pp. 1318–1325, 2023.

[13] D. Vance, M. Jin, T. Wenning, S. Nimbalkar, and C. Price, "Next-level energy management in manufacturing: Facility-level energy digital twin framework based on machine learning and automated data collection," *Energies*, vol. 18, no. 13, p. 3242, 2025.

[14] A. Massaro, N. Epicoco, G. Loseto, G. Starace, and C. A. Ardito, "Smart metering and hardware trojan electronic digital twin based on artificial intelligence," *IFAC-PapersOnLine*, vol. 59, no. 9, pp. 247–252, 2025.

[15] R. K. Seidu, G. K. Fobiri, E. K. Buami, J. Rani, B. Tawiah, and S. Jiang, "Energy efficiency in textile production: Strategies and solutions," in *Advances in Textile Materials and Processing Techniques for Sustainability*. Singapore: Springer, 2025.

[16] N. Sharma, B. Allardyce, R. Rajkhowa, A. Adholeya, and R. Agrawal, "A substantial role of agro-textiles in agricultural applications," *Frontiers in Plant Science*, vol. 13, p. 895740, 2022.

[17] B. Zorić, T. Matić, and Z. Hocenski, "Classification of biscuit tiles for defect detection using fourier transform features," *ISA Transactions*, vol. 125, pp. 400–414, 2022.

[18] A. Massaro, G. Dipierro, E. Cannella, and A. M. Galiano, "Comparative analysis among discrete fourier transform, k-means and artificial neural networks image processing techniques oriented on quality control of assembled tires," *Information*, vol. 11, no. 5, p. 257, 2020.

[19] T. G. Nakkina *et al.*, "Learnings graph-fourier spectra of textured surface images for defect localization," *Manufacturing Letters*, vol. 41, pp. 1568–1578, 2024.

[20] D. W. Schmidt *et al.*, "Machining specific fourier power spectrum profiles into plastics for high energy density physics experiments," *Fusion Science and Technology*, vol. 73, no. 3, 2018.

[21] A. Massaro and A. Ekuakille, "Analysis of magnetic field impact on nanoparticles used in nanomedicine and a measurement approach," *Measurement*, vol. 226, p. 114167, 2024.